

Supplementary Information

Hydration of Ferric Chloride and Nitrate in Aqueous Solutions: Water-mediated Ion Pairing Revealed by Raman Spectroscopy

Stephen M. Baumler, William H. Hartt V, and Heather C. Allen*

Department of Chemistry & Biochemistry, The Ohio State University,

100 West 18th Avenue, Columbus, Ohio 43210, United States

Experimental Methods

Table S1: Ratio of water molecules to dissolved ionic species for the ferric chloro- and nitrate solutions.

<i>Molality (mol/kg)</i>	<i>Molarity (mol/L)</i>	<i>Mol%</i>	<i># of Water assuming complete dissociation</i>
0.05	0.05	0.2	76
0.1	0.1	0.4	38
0.2	0.2	0.7	19
0.3	0.3	1.1	13
0.4	0.4	1.4	10
0.5	0.5	1.8	8
0.6	0.6	2.1	6

Table S1 shows the relationship between the molality of the prepared solutions and additional composition ratios including molarity and mol %. The number of waters to each on assuming complete dissociation of the salt into four ionic species is also shown.

Table S2: pH values of prepared solutions.

<i>[Fe]</i>	<i>pH FeCl₃</i>	<i>pH Fe(NO₃)₃</i>
0.00	5.6	5.6
0.05	2.2	2.2
0.10	1.9	1.8
0.20	1.6	1.4
0.30	1.4	1.2
0.40	1.3	1.0
0.50	1.2	0.9
0.60	1.1	0.8

a. All pH values were measured to be accurate within 0.1 units ($\pm 1\sigma$)

Table S2 shows the measured concentration dependent pH values for the ferric chloride and ferric nitrate solutions. pH values are the result of averaging three independently prepared solutions and were not observed to change over a 24hr period.

1. Collection of Experimental Polarized Raman Spectra

Vertically polarized excitation light (532 nm) is first scattered off the sample. The vertically polarized and horizontally polarized (90° from incident polarization) is collected in a 180° geometry from the initial excitation orientation. Sample spectra are subtracted from the spectra of the empty sample compartment.

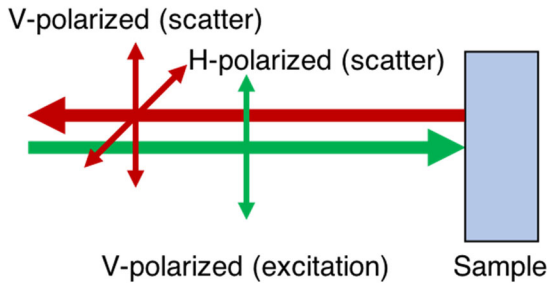


Figure S1: Excitation and collection light positioned in a 180° experimental geometry. Excitation light is polarized vertically (V) and the polarization of the scattered light is collected in both horizontal (H) and vertical (V) polarizations.

Due to both the geometry and polarization of the excitation and collected light, the observed spectra are proportional to:¹

$$H = 3\beta^2 \quad (1)$$

$$V = 45\alpha^2 + 4\beta^2 \quad (2)$$

where α^2 (isotropic) and β^2 (anisotropic) are the invariants of the Raman polarizability tensor. This leads to the calculation for the purely isotropic and anisotropic spectra by:

$$I^{iso}(\omega) = V(\omega) - (4/3)H(\omega) = 45\alpha^2(\omega) \quad (3)$$

$$I^{aniso}(\omega) = (4/3)H(\omega) = 4\beta^2(\omega) \quad (4)$$

2. Calculation of the Perturbed Water Spectrum

The perturbed water spectrum (**PWS**) is calculated as a bilinear decomposition of the data matrix D (where column 1 = the pure solvent spectrum, and column 2 = the solute + solvent spectrum) into the pure response spectral matrix S^T (where column 1 = the pure solvent spectrum, and column 2 = the pure solute spectrum) due to perturbation by a change in concentration C matrix.

$$D = CS^T + E \quad (5)$$

E is the matrix of residuals not explained by the linear model. **MCR-ALS** iteratively solves Eq. 5 by alternating least squares method calculating C and S^T while fitting to D using the initial estimates for C .

The **MCR-ALS** algorithm has 2 principle constraints:

1. Spectral non-negativity (using a Fast Non-negativity Least Squares (**FNNLS**) algorithm)
2. Closure: The sum across the row of the concentration matrix = 1.

For more details on the mathematics of the alternating least squares method and **FNNLS** algorithm please see references ²⁻³.

Supplemental Results

1. Preparation of the relative species abundance plot - Figure 1 in the parent manuscript.

Table S3: Average formation constants for the iron species collected from the literature.

	-log	Refs.
$[\text{Fe}(\text{H}_2\text{O})_6]^{3+} = [\text{Fe}(\text{H}_2\text{O})_5(\text{OH})]^{2+} + \text{H}^+$	$\log^*K_1 = -2.4 \pm 0.3$	4-11
$[\text{Fe}(\text{H}_2\text{O})_6]^{3+} = [\text{Fe}(\text{H}_2\text{O})_4(\text{OH})_2]^{+} + 2\text{H}^+$	$\log^*\beta_{1,2} = -6.2 \pm 0.5$	4-10, 12
$[\text{Fe}(\text{H}_2\text{O})_6]^{3+} = [\text{Fe}(\text{H}_2\text{O})_3(\text{OH})_3]^{+} + 3\text{H}^+$	$\log^*\beta_{1,3} = -13.1 \pm 1.2$	4-7, 12
$2[\text{Fe}(\text{H}_2\text{O})_6]^{3+} = [\text{Fe}_2(\text{H}_2\text{O})_8(\text{OH})_2]^{4+} + 2\text{H}^+ + 2\text{H}_2\text{O}$	$\log^*\beta_{2,2} = -3.0 \pm 0.1$	4-7, 10
$3[\text{Fe}(\text{H}_2\text{O})_6]^{3+} = [\text{Fe}_3(\text{H}_2\text{O})_8(\text{OH})_4]^{5+} + 4\text{H}^+ + 6\text{H}_2\text{O}$	$\log^*\beta_{3,4} = -6.3$	4-5
$[\text{Fe}(\text{H}_2\text{O})_6]^{3+} + \text{Cl}^- = [\text{Fe}(\text{H}_2\text{O})_5\text{Cl}]^{2+} + \text{H}_2\text{O}$	$\log K_1 = 1.5 \pm 0.0(4)$	13-15
$[\text{Fe}(\text{H}_2\text{O})_6]^{3+} + 2\text{Cl}^- = [\text{Fe}(\text{H}_2\text{O})_4\text{Cl}_2]^{+} + 2\text{H}_2\text{O}$	$\log \beta_{1,2} = 1.4 \pm 0.5$	13-16
$[\text{Fe}(\text{H}_2\text{O})_6]^{3+} + 3\text{Cl}^- = [\text{Fe}(\text{H}_2\text{O})_2\text{Cl}_3]^{+} + 4\text{H}_2\text{O}$	$\log \beta_{1,3} = 0.5 \pm 0.4$	13-15
$[\text{Fe}(\text{H}_2\text{O})_6]^{3+} + 4\text{Cl}^- = [\text{FeCl}_4]^{-} + 6\text{H}_2\text{O}$	$\log \beta_{1,4} = -1.6 \pm 0.4$	13-14
$[\text{Fe}(\text{H}_2\text{O})_6]^{3+} + \text{NO}_3^- = [\text{Fe}(\text{H}_2\text{O})_6\text{NO}_3]^{2+} + \text{H}_2\text{O}$	$\log K_1 = 0.9 \pm 0.1$	17-20

All values are reported as an average of the literature values. Error is reported as $\pm 1\sigma$.

Table S3 adopts the formalism described by Stumm and Morgan²¹ and shows the thermodynamic formation constants for the ferric hydrolysis, and complexed chloro- and nitrate species as an average obtained from the literature. The relative abundance of each ferric species is calculated using ChemEQL²² using the measured pH for each concentration (Table S2) and equilibrium constants from Table S3.

2. Supplemental electronic and vibrational spectra

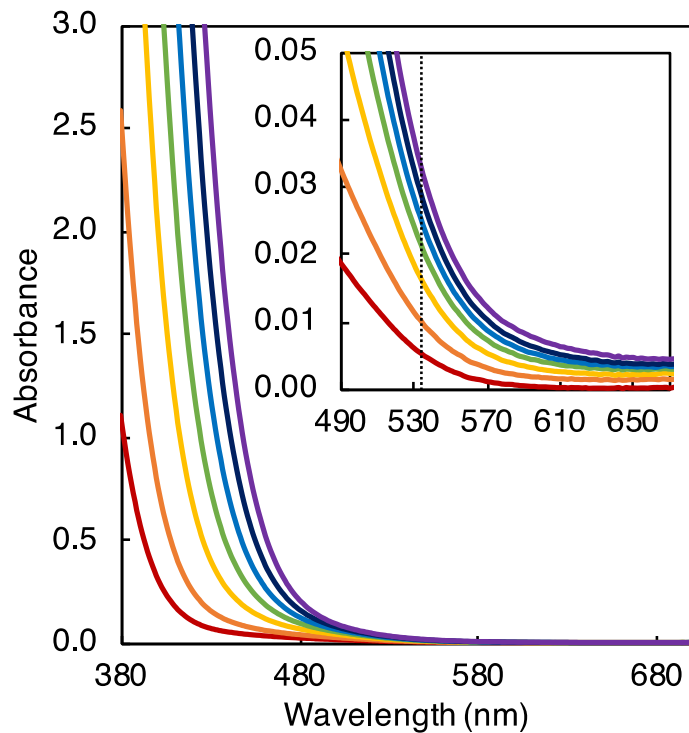


Figure S2: UV-Vis absorbance for the ferric chloride solution series: 0.05m (red) to 0.6m (purple). Spectra were background subtracted from water. Dotted line (inset) corresponds to the 532.2nm laser line used for the polarized Raman measurements.

Figure S2 shows the concentration dependent UV-Vis spectra for the ferric chloride solutions. There is intense absorbance at *ca.* 470 nm for the measured concentrations. There is a difference in the measured absorbance of *ca.* 0.03 absorbance units at the Raman line 532.2 nm over the concentrations measured.

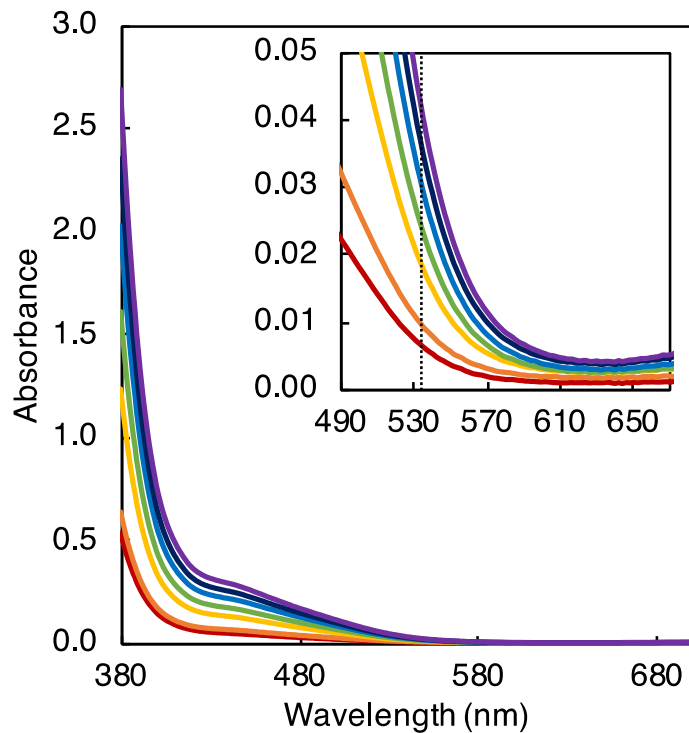


Figure S3: UV-Vis absorbance for the ferric nitrate solution series: 0.05m (red) to 0.6m (purple). Spectra were background subtracted from water. Dotted line (inset) corresponds to the 532.2nm laser line used for the polarized Raman measurements.

Figure S3 shows the concentration dependent UV-Vis spectra for the ferric nitrate solutions. There is intense absorbance at *ca.* 430 nm for the measured concentrations. The ferric nitrate salts exhibit a peak shoulder from *ca.* 430 to 570 nm. There is a difference in the measured absorbance of *ca.* 0.04 absorbance units at the Raman line 532.2 nm over the concentrations measured.

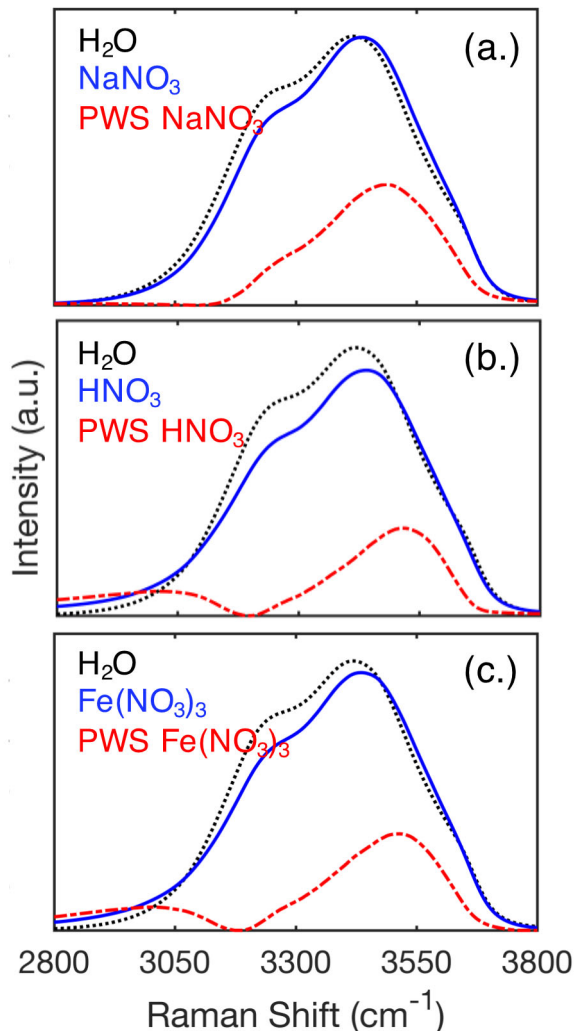


Figure S4: Unpolarized Raman spectra of (a.) 1.5m NaNO_3 , (b.) 1.5m HNO_3 , and (c.) 0.5m $\text{Fe}(\text{NO}_3)_3$. Perturbed water spectra are shown in red (dash-dot and are amplified x2 for clarity), and pure water spectrum in black (dot).

Figure S4 shows the measured unpolarized Raman spectra and PWS for 1.5m NaNO_3 , 1.5m HNO_3 , and 0.5m $\text{Fe}(\text{NO}_3)_3$ solutions. Comparisons to NaCl , HCl , and the ferric chloride solution are made in the parent text.

References

1. Scherer, J. R.; Kint, S.; Bailey, G. F., Spectral display of isotropic and anisotropic Raman scattering. *Journal of Molecular Spectroscopy* **1971**, *39*, 146-148.
2. de Juan, A.; Tauler, R., Multivariate Curve Resolution (MCR) from 2000: Progress in Concepts and Applications. *Critical Reviews in Analytical Chemistry* **2006**, *36*, 163-176.
3. de Juan, A.; Jaumot, J.; Tauler, R., Multivariate Curve Resolution (MCR). Solving the mixture analysis problem. *Anal. Methods* **2014**, *6*, 4964-4976.
4. Baes, C. F.; Mesmer, R. E., *The Hydrolysis of Cations*. John Wiley & Sons, Inc: New York, NY, 1976.
5. Smith, R. M.; Martell, A. E., *Critical Stability Constants*. 1976.
6. Stefánsson, A., Iron(III) Hydrolysis and Solubility at 25 °C. *Environ Sci Technol* **2007**, *41*, 6117-6123.
7. Liu, X.; Millero, F. J., The solubility of iron hydroxide in sodium chloride solutions. *Geochim Cosmochim Ac* **1999**, *63*, 3487-3497.
8. Lamb, A. B.; Jacques, A. G., The Slow Hydrolysis of Ferric Chloride in Dilute Solution. II. The Change in Hydrogen Ion Concentration. *J Am Chem Soc* **1938**, *60*, 1215-1225.
9. Khoe, G. H.; Brown, P. L.; Sylva, R. N.; Robins, R. G., The Hydrolysis of Metal-Ions .9. Iron(III) in Perchlorate, Nitrate, and Chloride Media (1 Mol Dm-3). *J Chem Soc Dalton* **1986**, 1901-1906.
10. Perrin, D. D., 338. The stability of iron complexes. Part IV. Ferric complexes with aliphatic acids. *Journal of the Chemical Society (Resumed)* **1959**, 1710-1717.
11. Milburn, R. M.; Vosburgh, W. C., A Spectrophotometric Study of the Hydrolysis of Iron(III) Ion. II. Polynuclear Species1. *J Am Chem Soc* **1955**, *77*, 1352-1355.
12. Turner, D. R.; Whitfield, M.; Dickson, A. G., The equilibrium speciation of dissolved components in freshwater and sea water at 25°C and 1 atm pressure. *Geochim Cosmochim Ac* **1981**, *45*, 855-881.
13. Liu, W.; Etschmann, B.; Brugger, J.; Spiccia, L.; Foran, G.; McInnes, B., UV-Vis spectrophotometric and XAFS studies of ferric chloride complexes in hyper-saline LiCl solutions at 25–90 °C. *Chem Geol* **2006**, *231*, 326-349.
14. Gamlen, G. A.; Jordan, D. O., A Spectrophotometric Study of the Iron(III) Chloro-Complexes. *J Chem Soc* **1953**, 1435-1443.
15. Stefánsson, A.; Lemke, K. H.; Sewar, T. M. In *Iron(III) complexation in hydrothermal solutions – An experimental and theoretical study*, 15th International Conference on the Properties of Water and Steam (ICPWS 15), Berlin, September 7-11, 2008; Span, R.; Weber, I., Eds. Verein Deutscher Ingenieure VDI: Berlin, 2008.
16. Strahm, U.; Patel, R. C.; Matijevic, E., Thermodynamics and Kinetics of Aqueous Iron(III) Chloride Complexes Formation. *J Phys Chem-Us* **1979**, *83*, 1689-1695.

17. Sykes, K. W., 26. The reaction between ferric and iodide ions. Part II. The influence of ionic association. *Journal of the Chemical Society (Resumed)* **1952**.
18. Mattoo, B. N., Stability of Metal Complexes in Solution. *Zeitschrift für Physikalische Chemie* **1959**, *19*, 156-167.
19. Ibers, J. A.; Davidson, N., On the Interaction between Hexacyanatoferate(III) Ions and (a) Hexacyanatoferate(II) or (b) Iron(III) Ions_{1a,2}. *J Am Chem Soc* **1951**, *73*, 476-478.
20. Horne, R. A.; Myers, B. R.; Frysinger, G. R., The Effect of Pressure on the Dissociation of Iron(III) Monochloride Complex Ion in Aqueous Solution. *Inorg Chem* **1964**, *3*, 452-454.
21. Stumm, W.; Morgan, J. J., *Aquatic Chemistry: Chemical Equilibria and Rates in Natural Waters*. 3rd ed.; Wiley: New York, 1996.
22. Müller, B.; Brassel, K.-H. *ChemEQL*, 3.2; Eawag: Swiss Federal Institute of Aquatic Science and Technology: 2015.